NeuroImage: Clinical 35 (2022) 103055

Contents lists available at ScienceDirect

NeuroImage: Clinical

journal homepage: www.elsevier.com/locate/ynicl

Edge-centric analysis of stroke patients: An alternative approach for biomarkers of lesion recovery

Sebastian Idesis [a,*], Joshua Faskowitz [b,c], Richard F. Betzel [b,c,d,e], Maurizio Corbetta [f,g,h,i,j], Olaf Sporns [b,c,d,e], Gustavo Deco [a,k]

[a] Center for Brain and Cognition (CBC), Department of Information Technologies and Communications (DTIC), Pompeu Fabra University, Edifici Mercè Rodoreda, Carrer Trias i Fargas 25-27, 08005 Barcelona, Catalonia, Spain
[b] Department of Psychological and Brain Science, Indiana University, Bloomington, IN 47405, United States
[c] Program in Neuroscience, Indiana University, Bloomington, IN 47405, United States
[d] Cognitive Science Program, Indiana University, Bloomington, IN 47405, United States
[e] Network Science Institute, Indiana University, Bloomington, IN 47405, United States
[f] Padova Neuroscience Center (PNC), University of Padova, via Orus 2/B, 35129 Padova, Italy
[g] Department of Neuroscience (DNS), University of Padova, via Giustiniani 2, 35128 Padova, Italy
[h] Department of Neurology, Washington University School of Medicine, 660 S. Euclid Ave, St. Louis, MO 63110, United States
[i] Department of Radiology, Washington University School of Medicine, 660 S. Euclid Ave, St. Louis, MO 63110, United States
[j] VIMM, Venetian Institute of Molecular Medicine (VIMM), Biomedical Foundation, via Orus 2, 35129 Padova, Italy
[k] Institució Catalana de Recerca I Estudis Avançats (ICREA), Passeig Lluis Companys 23, 08010 Barcelona, Catalonia, Spain

ARTICLE INFO

Keywords:
Stroke
Edge-centric
Functional connectivity
Entropy
Brain dynamics
Longitudinal

ABSTRACT

Most neuroimaging studies of post-stroke recovery rely on analyses derived from standard node-centric functional connectivity to map the distributed effects in stroke patients. Here, given the importance of nonlocal and diffuse damage, we use an edge-centric approach to functional connectivity in order to provide an alternative description of the effects of this disorder. These techniques allow for the rendering of metrics such as normalized entropy, which describes the diversity of edge communities at each node. Moreover, the approach enables the identification of high amplitude co-fluctuations in fMRI time series. We found that normalized entropy is associated with stroke lesion severity and continually increases across the time of patients' recovery. Furthermore, high amplitude co-fluctuations not only relate to the lesion severity but are also associated with patients' level of recovery. The current study is the first edge-centric application for a clinical population in a longitudinal dataset and demonstrates how a different perspective for functional data analysis can further characterize topographic modulations of brain dynamics.

1. Introduction

The brain can be conceptualized as a system of regions that functionally influence each other, forming a complex network of interactions (Bassett and Sporns, 2017; Park and Friston, 2013). Stroke causes focal brain lesions that alters this network organization both locally and globally (Crofts et al., 2011; Wang et al., 2019). The tools of network science and graph theory allow for these changes to be quantified in various ways. Using functional magnetic resonance imaging (fMRI), it has been shown that the functional synchronization between distinct regions of the brain, referred to as functional connectivity (FC), is disrupted by stroke (Silasi and Murphy, 2014; Wodeyar et al., 2020). Commonly observed disruptions to this network organization include inter- and intra-hemispheric changes in FC (Crofts et al., 2011; Griffis et al., 2019a; Siegel et al., 2016). Furthermore, using structural magnetic resonance imaging (sMRI) of the brain's white matter architecture, several studies have shown how structural disconnections explain brain network (such as modularity and synchronization) dysfunction after stroke (Corbetta et al., 2015; Griffis et al., 2019b; Siegel et al., 2016; Wang et al., 2019). These studies show how decreases in modularity and synchronization are strongly related to behavioral deficits.

Common to many network neuroscience investigations is a reliance on network analyses that result in measurements specific to each brain region. A recent study proposed that resting-state functional

* Corresponding author.
E-mail addresses: sebastian.idesis@upf.edu, sebastian.idesis@gmail.com (S. Idesis).

https://doi.org/10.1016/j.nicl.2022.103055
Received 4 February 2022; Received in revised form 19 May 2022; Accepted 21 May 2022
Available online 23 May 2022

connectivity (rsFC) may not be fully representative of brain activation patterns underlying specific behaviors, which was shown to be constrained by the structural connectome (Honey et al., 2007; Honey et al., 2009; Olafson et al., 2021). Therefore, it could be the case that the observed modulations of functional connectivity following stroke represent an incomplete picture of the brain dysfunction linked to ipsi- and contralateral stroke. Along these lines, new analytical approaches should be explored to see if they can further expand our understanding of these fMRI-derived modulations. In particular, new network-based analyses of fMRI that focus on the brain's functional connections, known as edges, could help to fill these gaps.

Recent studies have motivated an edge-centric approach, shifting focus onto the information that can be resolved on a per-edge level (Ahn et al., 2010; Faskowitz et al., 2020; Zamani Esfahlani et al., 2020). Using a straightforward unwrapping of the Pearson correlation, co-fluctuation time series (alternatively referred to as "edge time series") data can be estimated for each edge. Unlike sliding-window time-varying connectivity, which requires the parameterization of a window duration, kernel shape, and step size, edge time series have the same temporal resolution as the original functional data. Importantly, the time-averaged value of an edge time series is a correlation coefficient. This means that edge time series are a mathematically exact decomposition of a functional connection into its framewise contributions. Previous analyses of edge time series data have shown that transient periods of high-amplitude activity make disproportionately large contributions to the time-averaged functional connectivity (Allan et al., 2015; Cifre et al., 2020; Petridou et al., 2013; Tagliazucchi et al., 2012; Zamani Esfahlani et al., 2020). In other words, data selected from specific temporal slices can be used to reconstruct a similarity matrix with a high correspondence to the functional connectivity matrix constructed from the full dataset (Betzel et al., 2021; Greenwell et al., 2021). Like with co-activation pattern (CAP) analysis (Karahanoglu and Van De Ville, 2015; Liu and Duyn, 2013), the structure of high-amplitude activity forms distinctive spatial patterns that are transiently expressed and only partly resembles the canonical functional systems architecture (Sporns et al., 2021). What separates edge time series from previous methods is that it provides an exact mathematical relationship to the Pearson correlation.

Edge time series can be compared in a pairwise manner, creating an edge-by-edge similarity matrix of the brain that can be submitted to network analyses. Clustering this data results in a community structure of edges, where communities represent groups of region pairs that similarly fluctuate across time (Chumin et al., 2021; Jo et al., 2021b). When mapped to brain regions, these edge communities naturally form a pervasively overlapping structure, such that every node participates in multiple communities. The distribution of edge community affiliations can be conceptualized as an entropy that describes how dispersed the edge community distribution is at each node. Up until this point, this family of approaches has been applied to map fMRI data from young and healthy samples. Consequently, these approaches have not yet been applied to measure the impact of neural dysfunction and/or damage.

In the present study we explore the utility of edge-centric analytical approaches in a clinical setting, by using newly developed measures that disclose information at the edge level. More specifically, we measure the relation between edge-centric derived measures and metrics of post-stroke severity and classification. Additionally, this study examines how these edge measurements possibly change across time, in a longitudinal neuroimaging setting and its association with the level of patients' recovery. In this work, we used the Washington University Stroke Cohort dataset (Corbetta et al., 2015), a large longitudinal (2 weeks, 3 months, 12 months) study of heterogeneous first-time single strokes that contains in-depth neuropsychological measures of multiple functions and multimodal imaging data. From this cohort we selected 96 S patients and 27 healthy subjects for the longitudinal analyses (See more in Methods). We found that normalized entropy of the edge community distributions increased globally across the time, as patients recovered from stroke. Furthermore, we found that a marker of high amplitude co-fluctuation has a significant relation with lesion volume and an association with the patients' recovery after 1 year. In summary, the current study reveals how edge-centric analysis provides indicators that reveal lesion severity and reflect lesion recovery, making it the first study with edge-centric approach with clinical applications across time.

2. Methods

2.1. Sample (Cohort 1)

The database includes patients with first-time stroke, studied 1–2 weeks (mean = 13.4 days, SD = 4.8 days), 3 months, and 12 months after stroke onset. Also, a group of 27 age-matched control subjects was evaluated twice at an interval of 3 months.

2.1.1. Stroke patients

Subjects (n = 96) were recruited from the stroke service at Barnes-Jewish Hospital (BJH), with the help of the Washington University Cognitive Rehabilitation Research Group (CRRG). The complete data collection protocol is described in full detail in previous publication (Corbetta et al., 2015).

2.1.2. Healthy

27 controls were selected based on the same inclusion/exclusion criteria of the study (Corbetta et al., 2015). This group was typically constituted by spouses or first-degree relatives of the patients, age- and education-matched to the stroke sample.

2.2. Sample (Cohort 2)

Data from a replication sample was acquired as part of the Washington University Stroke Cohort (See section below) and therefore processed in a nearly identical manner. The only difference in the replication sample's image processing workflow was the application of distortion correction of the fMRI using gradient echo field maps. The replication cohort is composed of 10 S patients and 10 healthy controls.

2.3. fMRI data acquisition and preprocessing

We use data from the Washington University Stroke Cohort, extensively described in previous articles (Corbetta et al., 2015; Siegel et al., 2016; Siegel et al., 2018). A brief description of the data acquisition and preprocessing follows. A complete description of it is explained in detail in a previous publication (Griffis et al., 2019).

Neuroimaging data were collected at the Washington University School of Medicine using a Siemens 3 T Tim-Trio scanner with a 12-channel head coil. It was obtained sagittal T1-weighted MP-RAGE (TR = 1950 msec; TE = 2.26 msec, flip angle = 90 degrees; voxel dimensions = 1.0 × 1.0 × 1.0 mm), and gradient echo EPI (TR = 2000 msec; TE = 2 msec; 32 contiguous slices; 4x4 mm in-plane resolution) resting-state functional MRI scans from each subject. Participants were instructed to fixate on a small centrally-located white fixation cross that was presented against a black background on a screen at the back of the magnet bore. Between six and eight resting-state scans (128 volumes each) were obtained from each participant (~30 min total) giving a total of 896 time points for each participant.

Resting-state fMRI preprocessing included (i) regression of head motion, signal from ventricles and CSF, signal from white matter, global signal (ii) temporal filtering retaining frequencies in 0.009–0.08 Hz band; and (iii) frame censoring, FD = 0.5 mm. Finally, the resulting time series were projected on the cortical and subcortical surface of each subject divided into the 235 ROIs (200 cortical plus 35 subcortical).

These areas are taken from the multi-resolution functional connectivity-based cortical parcellations developed by Schaefer and colleagues (Schaefer et al., 2018), including additional subcortical and cerebellar parcels from the Automated Anatomical Labeling (AAL) atlas

(Tzourio-Mazoyer et al., 2002) and a brainstem parcel from the Harvard-Oxford Subcortical atlas (https://fsl.fmrib.ox.ac.uk/fsl/fslwiki/Atlases).

2.4. Stroke deficit assessment

2.4.1. Lesion severity (Lesion volume)

Lesion severity was calculated based on the topography of stroke using a voxel-wise analysis of structural lesions. Each lesion was manually segmented on structural MRI scans and checked by two board certified neurologists. The location (cortico-subcortical, subcortical, white-matter) of each individual lesion was assigned with an unsupervised K-means clustering on the percentage of total cortical/subcortical gray and white matter masks overlay. The overlap of each lesion group with gray matter, white matter and subcortical nuclei is explained in detail in a previous publication (see (Corbetta et al., 2015)).

We summarize the lesion distribution and average of the used sample in Sup. Fig. 7.

2.4.2. Neuropsychological testing

As reported in a previous work (Corbetta et al., 2018), the same subjects (controls and patients) were also examined at each time point through a battery of neuropsychological tests in the domains of motor, attention, language, visual, and memory functions. Imaging and behavioral testing sessions were almost always performed on the same day. Scores were only recorded for tasks that subjects were able to complete. Dimensionality reduction was applied to the performance data using principal component analysis as described in detail in a previous publication (Corbetta et al., 2015). In other words, PCA was run on each category and the first component was used as a domain score. Finally, patients' behavioral scores were z-scored with regards to controls' scores, to highlight behavioral impairments.

2.4.3. Stroke symptoms (NIHSS Score)

In addition to aforementioned domain-specific scores, the patients' clinical severity was assessed through the National Institutes of Health Stroke Scale (NIHSS) (Brott et al., 1989), which includes 15 subtests addressing: level of consciousness (LOC), gaze and visual field deficits, facial palsy, upper and lower motor deficits, limb ataxia, sensory impairment, inattention, dysarthria and language deficits.

Studies on the factor structure of the NIHSS (Lyden et al., 2004; Zandieh et al., 2012) capture the great majority of variability in performance (Corbetta et al., 2015). The total NIHSS was used as an averaged measure of the clinical severity for each patient.

2.5. Edge-centric calculations: Normalized entropy and high amplitude co-fluctuations

Time series were extracted for each node (N = 235 brain regions) of the parcellation by averaging the preprocessed fMRI BOLD signal within each node at each timepoint. Taking the statistical similarity, as commonly indexed by Pearson correlation, between each possible pair of nodal time series would result in a N-by-N (235-by-235) similarity matrix. This matrix is commonly referred to as a functional connectivity matrix. Recently, a new method has been proposed to represent the time series formed by comparing two nodes, by using an intermediate calculation of the Pearson correlation (Faskowitz et al., 2020; Zamani Esfahlani et al., 2020). The resulting edge time series are formed by first, z-scoring each of the two nodal time series independently. Then, the element-wise product of the z-scored time series is taken, forming an edge time series. Values of the edge time series reflect the co-fluctuation pattern between nodes. A positive co-fluctuation results when, at a specific point in time, both series are concordant relative to each of their mean signals. A negative co-fluctuation value results when, at a specific point in time, one time series is above the mean (a positive value) and the other is below the mean (a negative value). Notably, the mean of an edge time series equals the Pearson correlation.

Edge time series have the same temporal resolution as the original data, allowing for the analysis of instantaneous (i.e., a single time frame) co-fluctuation patterns. This data has the dimensionality of edge-by-time. At each frame, the overall co-fluctuation activity can be indexed by taking the root-sum-square (RSS) of all edge co-fluctuations. Then, using these RSS values, the time frames can be ranked. Here, we grouped time frames into 10 ordered deciles based on RSS co-fluctuation activity.

Edges can be clustered based on the similarity of their time course. Here, we applied the k-means algorithm (normalized Euclidean distance metric) to partition the set of edges into 10 clusters with similar co-fluctuation amplitude. The number of clusters was set to match the presented results in a previous paper (Faskowitz et al., 2020). K-means was repeated 25 times and the partition that was least distant from all other clusters (as assessed by minimum variation of information) was taken to be the representative solution for a given dataset (Faskowitz et al., 2018). This procedure results in a community affiliation for each edge. That is, each edge is associated with one of k communities, where k is 10. By projecting this partition to the node level, we find that the 234 edges (excluding self-loops; therefore N-1) emanating from each node are affiliated with edge communities. Summing edge communities of each node and dividing by 234 provides a probability distribution over the k communities. We can then take the entropy of this distribution, to obtain a measurement of how dispersed the distribution of edge clusters are at each node. A low entropy indicates a relatively even distribution of edge communities associated with a node, whereas a high edge community indicates a high concentration in relatively few communities. Here, we employ the normalized entropy, which is bounded between the interval [0,1].

2.6. Entropy localization

The difference between patients and controls was calculated for each node and then displayed in the brain surface plot (Fig. 3a).

2.7. Functional system interactions

To investigate the average correlations between canonical functional networks, we compared the within and between network average FC for both patients and controls at the three distinct timepoints. The sum of weights of the connections between the networks was then Fisher z-transformed to be compared between them at the same scale expressing the co-activity of these networks after the stroke damage and this co-activity recovered across time. The connections displayed exceed the chosen threshold of 1.75 to emphasize the effect (Fig. 3b).

2.8. Participation coefficient

We calculated the participation coefficient within each time window for each node using the Brain Connectivity Toolbox (BCT) (https://sites.google.com/site/bctnet/) (Rubinov and Sporns, 2010) function "participation_coef_sign.m", averaging across 500 trials of modularity maximization with the "negative_asym" null model option (Rubinov and Sporns, 2011). The participation coefficient in this study expresses the level at which a node is diversely associated with other nodes across all modules (Fukushima et al., 2018; Rubinov and Sporns, 2010). The (node) modules used for the participation coefficient were obtained by using the modularity undirected function (community detection technique from the BCT). As the normalized entropy did not reveal a significant relation with lesion metrics in an individual level at the acute stage of the injury, participation coefficient was calculated given its previous importance in the field (Warren et al., 2014).

2.9. High amplitude co-fluctuations: similarity with FC and principal component analysis

Using the RSS to sort the data (see Edge-centric calculations section),

we calculated a similarity matrix by averaging the top 10% RSS frames. The elements of this matrix represent the cofluctuation patterns that are expressed when the brain is a high-amplitude state (i.e.: the first decile as ranked by RSS). The chosen decile was based on previous literature (Zamani Esfahlani et al., 2020) while a comparison between the different deciles is described in Fig. S4. The obtained similarity matrix was then compared to the full FC matrix (calculated from all frames) using the Pearson correlation (of the vectorized upper triangle for each matrix). This resulted in a coefficient for each subject, representing the similarity between a subject's high-amplitude values and the FC. This value was associated with lesion volume and used to reveal the number of recovered domains (Fig. 5a) and to be compared with the lowest 10% scores (Fig. 5b). Additionally, we calculated the first principal component (PC) of each edge time series matrix, for each patient, at the three different timepoints. This singular value partially describes the first axis of the edge-time series variance. With this addition, we can inspect and compare our results against a node-centric approach as discussed in previous literature (Novelli and Razi, 2021).

2.10. Classification between left vs right hemisphere

The normalized entropy calculation was performed in parallel for two subsets of patients according to the location of the stroke: 49 left hemisphere lesioned patients and 47 right hemisphere lesioned patients. In this way, the two groups were compared based on the entropy levels of the patients belonging to the corresponding subset. No classification model was assessed for this comparison. Supplementary Table 1 summarizes the Lesion volume and NIHSS of the groups presented in this analysis.

2.11. Classification between subcortical vs cortical region

The normalized entropy calculation was performed in parallel for two subsets of patients according to the location of the stroke, with 33 patients with cortical area lesions and 23 patients with subcortical area lesions. For remaining patients, the lesion location was unspecific or a combination of both tissue areas. As in the previous section, the entropy level of the subjects of each sample (in this case, patients with cortical vs patients with subcortical lesion) was compared to the other one without

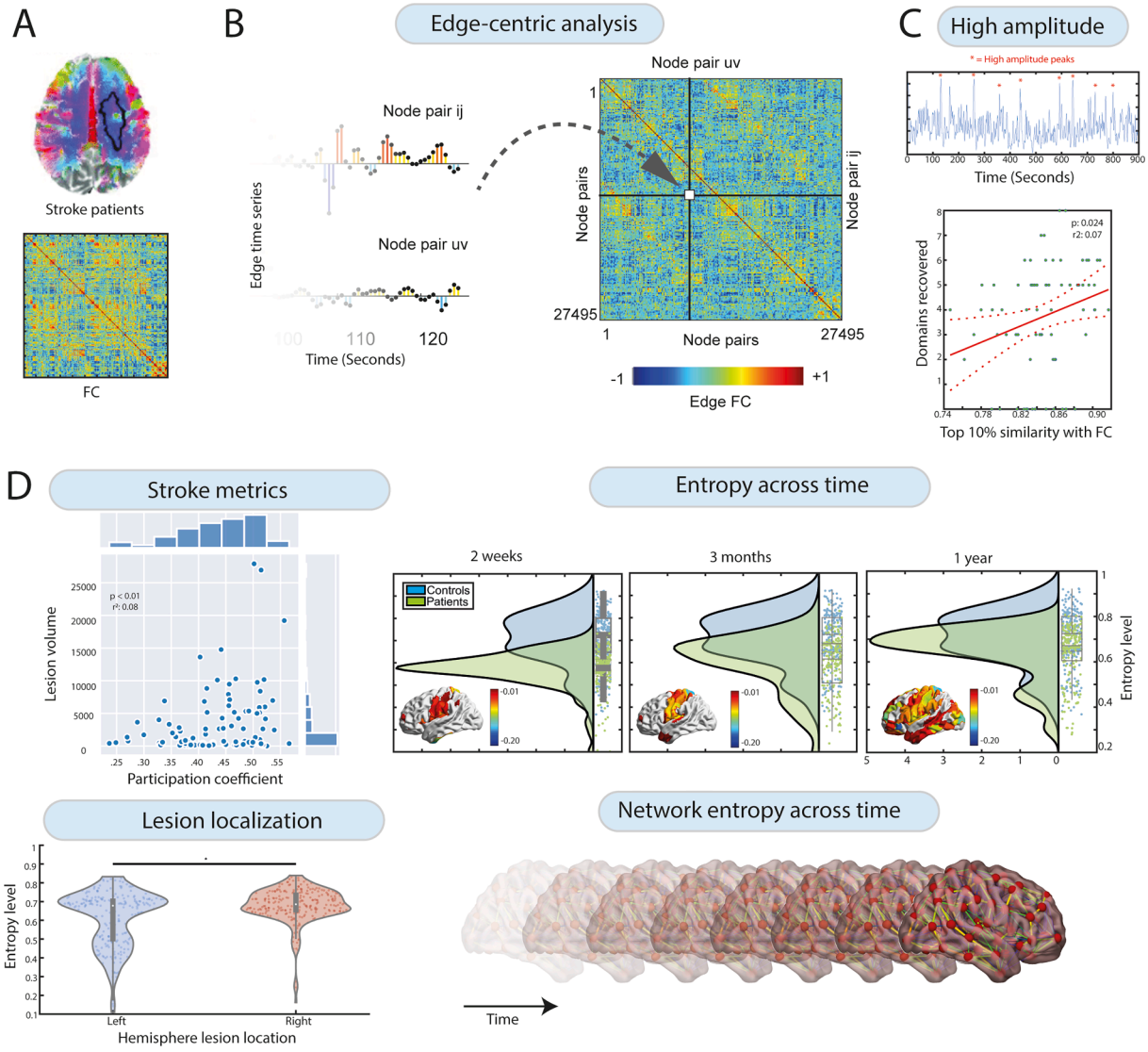

Fig. 1. Pipeline: (A) All the analysis were performed using the FC of the stroke patients. (B) Edge-FC is calculated by multiplying element-wise the product time series and normalizing the sum by the squared root standard deviations of both time series. (C) The elements of the co-fluctuation time series are the element-wise products of z-scored regional BOLD time series, from which the highest peaks are selected for further analysis. (D) Normalized entropy and participation coefficient were obtained in order to assess their fluctuation across time, their relation with stroke metrics and their collaboration with lesion localization.

performing a classification model. Supplementary Table 1 summarizes the Lesion volume and NIHSS of the groups presented in this analysis.

3. Results

We performed a series of analyses on the functional MRI data of stroke patients (Fig. 1a). The first step consisted in obtaining the edge-time series (Fig. 1b) which was calculated for the three distinct time-points. After calculating co-fluctuation amplitude, the data was sorted and segmented to obtain the 10% of frames with the highest co-fluctuation amplitude (Fig. 1c). Lastly, the edge community entropy was calculated per node to observe its relationship with stroke metrics, its relation with the lesion localization and its fluctuation across time both by node and network (Fig. 1d).

To measure the effect of time, we compared the first principal component (PC) singular value for each patient at the three different timepoints. There was not a significant effect of time on the first PC ($F(2,147) = 0.08$, $p = 0.91$). All p-values reported in the results section were corrected using False Discovery Rate. The same effect was observed on the top 10% high-amplitude values ($F(2,132) = 0.47$, $p = 0.62$). There was a significant difference when comparing the level of entropy at the three different time points [$F(2,702) = 30.64$, $p < 0.01$]. Timepoint 3 showed the highest value (mean = 0.74, sd = 0.11) followed by timepoint 1 (mean = 0.68, sd = 0.11) and timepoint 2 (mean = 0.67, sd = 0.14) (Fig. 2). Entropy level revealed an increasing trend across time that was not apparent in the other two metrics. Based on these results, we selected normalized entropy as the variable of interest to be used as a potential fMRI-based indicator of recovery by comparing it with the corresponding values in the control group (Fig. 3a).

In order to investigate the difference in entropy levels between controls and patients, we compared both groups at each time point. There was a significant difference between patients and controls at time

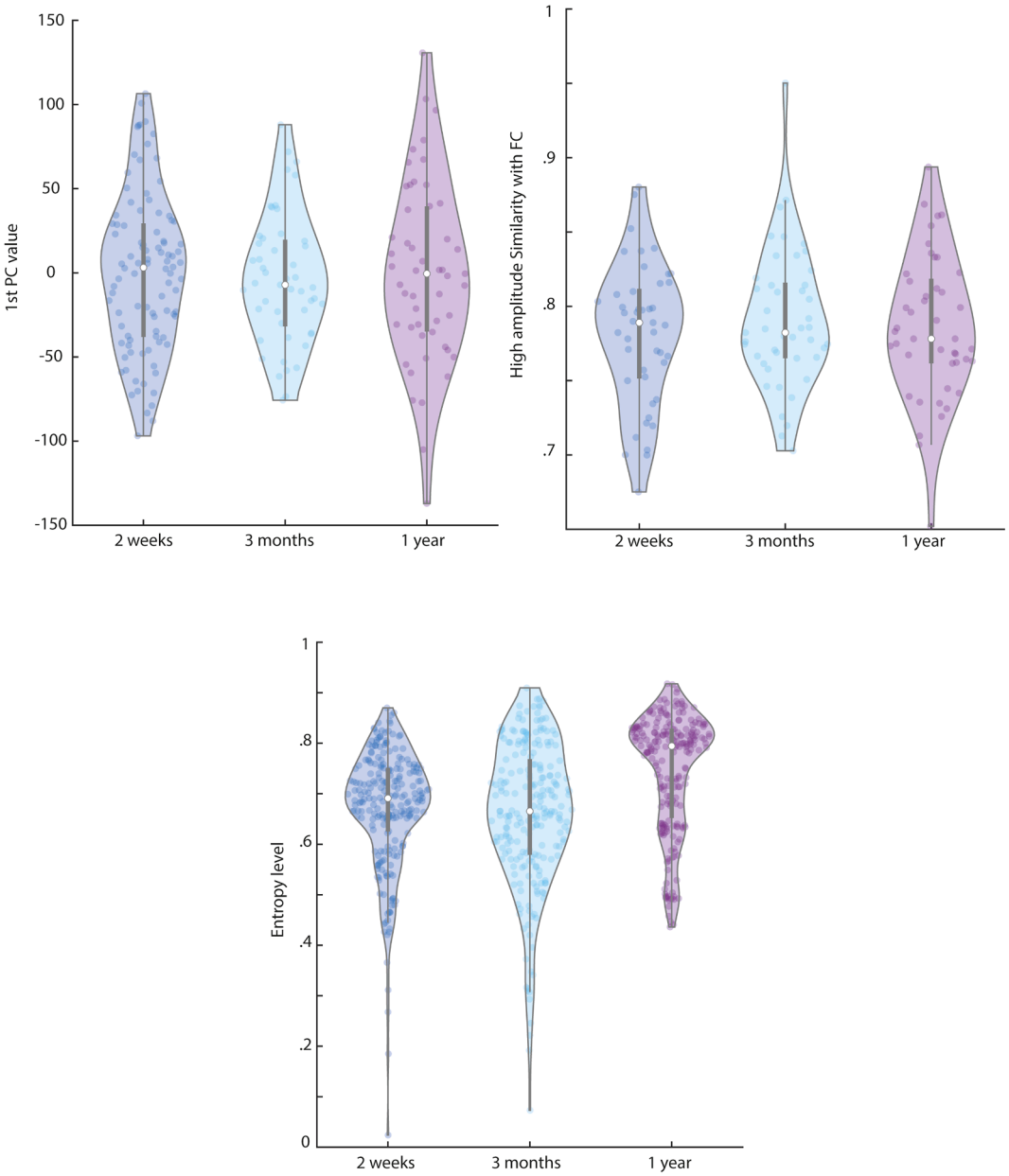

Fig. 2. Fluctuation across time of principal components, high amplitude co-fluctuations, and entropy. Representation of participants' values at three different time points after stroke (2 weeks, 3 months, and 1 year) for (top-left) the first PC of static nFC, (top-right) high-amplitude similarity with FC and (bottom) the entropy level.

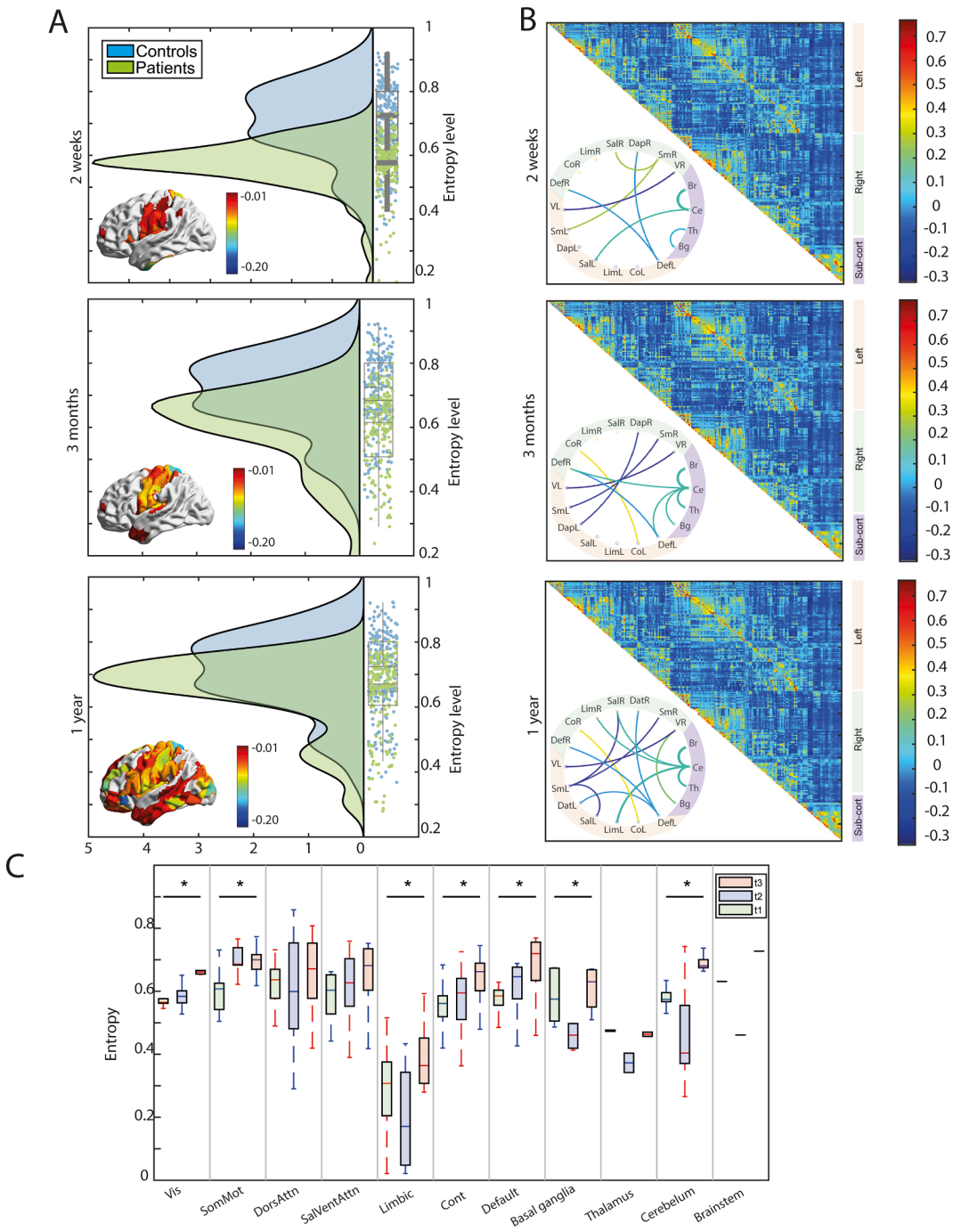

Fig. 3. Entropy and FC across time: (A) Comparison of entropy between patients and control at each time point. The difference is visualized in each surface for each node. (B) FC at each timepoint with the corresponding communication between the networks. (C) Entropy across time segmented by network. Asterisk indicates when the comparison between the three time points is significant. Systems labels: V = Visual; Sm = Somato-motor; Dat = Dorso-attentional; Sal = Salience; Lim = Limbic; Co = Control; Def = Default; Bg = Basal Ganglia; Th = Thalamus; Ce = Cerebellum; Br = Brainstem.

point 1 ($t(468) = 13.78$, $p < 0.01$), timepoint 2 ($t(468) = 10.86$, $p < 0.01$) and time point 3 ($t(468) = 5.45$, $p < 0.01$) with the magnitude of the difference between the two groups decreasing over time (Fig. 3a). The increase in normalized entropy and the reduced difference with the control group across time could be interpreted as an indication of recovery.

When visualizing the difference between patients and controls by node, there were 83 nodes in which the patients had a higher value than the controls in the acute stage (time point 1), 68 at time point 2, and 169 at time point 3 (Fig. 3a). We explored the surface projection of entropy values for each group and both combinations of differences (controls minus patients and patients minus controls) to observe both patterns (Supplementary Fig. 1). The localization of differences to individual nodes could prompt future exploration of this topographic pattern. Especially meaningful might be to explore the relationship between these maps and maps that index other topographic properties of the brain including cortical expansion or gene expression.

When visualizing the average functional correlation between the networks, 8 connections were preserved at time point 1, 10 connections at time point 2 and 14 connections at time point 3 (Fig. 3b) indicating the recovery of the patients across time.

To analyze the within-network fluctuation of the entropy level, we

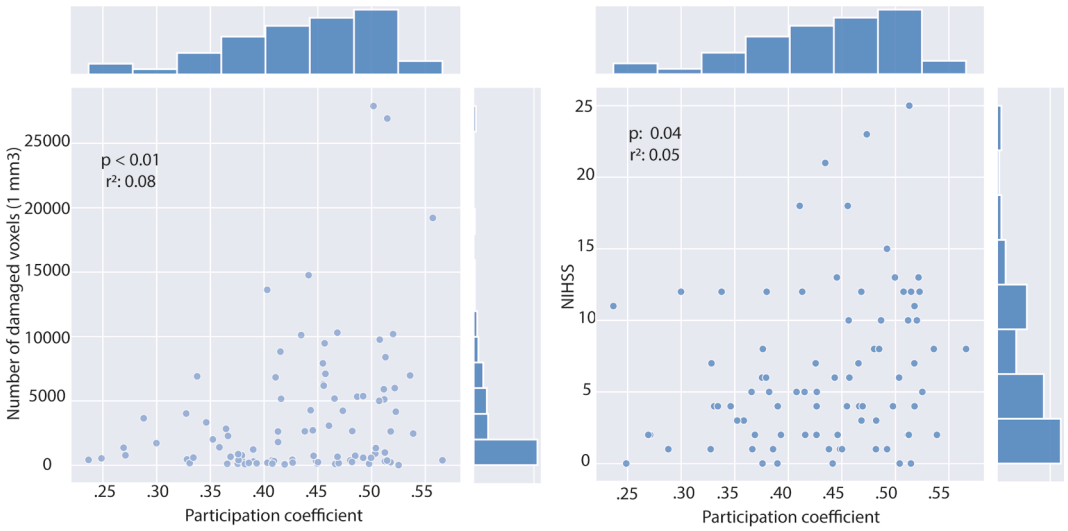

Fig. 4. Relation of Participation coefficient with stroke metrics: Relationship between the participant coefficient of each patient, (left) their lesion volume (Number of damaged voxels) and (right) their NIHSS score. Lesion volume was calculated based on the topography of the stroke damage using a voxel-wise analysis of structural lesions in order to quantify the amount of damaged voxels. The National Institutes of Health Stroke Scale (NIHSS) includes 15 subtests and was used as a clinical measure of severity for each patient.

compared it for each individual network. Several of them revealed a significant difference across time: Visual ($F(2,84) = 6.21$, $p < 0.01$), Somato-Motor ($F(2,102) = 77.45$, $p < 0.01$), Limbic ($F(2,33) = 5.87$, $p < 0.01$), Control ($F(2,87) = 4.72$, $p = 0.01$), Default ($F(2,135) = 13.57$, $p < 0.01$), Basal ganglia ($F(2,15) = 9.26$, $p < 0.01$) and Cerebellum ($F(2,75) = 39.3$, $p < 0.01$). In contrast, the remaining ones did not expose a significant difference between the different timepoints: Dorsal-Attention ($F(2,75) = 1.58$, $p = 0.21$), Salience-Ventral ($F(2,63) = 1.47$, $p = 0.23$), Thalamus ($F(2,3) = 9.43$, $p = 0.05$), Brainstem ($F(2,1) = 1.32$, $p = 0.36$) (Fig. 3c). The majority of the networks revealed an increase across time, indicating that the phenomena could be studied in both global and local ways.

Normalized entropy was found to be negatively associated with stroke metrics although these relations were not significant (lesion volume: $R^2 = 0.02$, $p = 0.37$, NIHSS score: $R^2 = 0.05$, $p = 0.163$) (Supplementary Fig. 2a). Therefore, the participation coefficient was explored as it was shown to have a strong statistical relationship with normalized entropy (Faskowitz et al, 2020).

The participation coefficient was calculated for each patient in order to see its correspondence with the basic stroke severity metrics. Average participation coefficient was related in a significant manner with the lesion volume ($R^2 = 0.08$, $p < 0.01$). The same occurred for the NIHSS score ($R^2 = 0.05$, $p = 0.04$) (Fig. 4). Furthermore, the participation coefficient relation with the stroke metrics was also analyzed in the other two time points showing no significant effect (timepoint 2: lesion volume: $R^2 = 0.04$, $p = 0.13$, NIHSS score: $R^2 = 0.01$, $p = 0.63$, timepoint 3: lesion volume: $R^2 = 0.01$, $p = 0.47$, NIHSS score: $R^2 = 0.01$, $p = 0.42$) indicating that this effect is only visible at the acute stage (Supplementary Fig. 2b). When comparing participation coefficient between patients and controls, no difference was found for any of the 3 timepoints (Supplementary Fig. 3) as opposed to the increasing trend exposed previously by normalized entropy.

The level similarity of the highest 10% data points (ranked by the RSS. For more detail see methods section) with the FC were associated with a significant percentage of the lesion volume ($R^2 = 0.05$, $p = 0.03$). Furthermore, they relate to a significant number of domains recovered ($R^2 = 0.07$, $p = 0.02$) (Fig. 5a). When comparing the correlation with the complete FC, the top 10% data points showed a significantly higher correlation value than the bottom 10% ($t(190) = 39.31$, $p < 0.01$)) (Fig. 5b). We explored the correlation of each decile of data points (i.e.: first 10%, 10% to 20%, and so on) to show the decaying effect of the correlation with the FC (Supplementary Fig. 4a). Furthermore, when compared to the other deciles, the highest 10% revealed to have the highest clustering coefficient, global efficiency and assortativity, next to the lowest distance (Supplementary Fig. 4b). The relation between each decile with lesion volume revealed that the only decile with a significant relation is the top 10% ($R^2 = 0.05$, $p = 0.03$) while all the others present no significant association ($p > 0.2$) (Supplementary Fig. 5).

When comparing patients' entropy level according to lesion localization, we found a significant difference between patients with cortical lesions (M = 0.74, SD = 0.12) when compared with the ones with subcortical ones (M = 0.68, SD = 0.12) ($t(468) = -5.13$, $p < 0.01$). In the same way, there is a significant difference between patients with right hemisphere lesions (M = 0.67, SD = 0.09) when compared with the ones with left hemisphere ones (M = 0.60, SD = 0.14) ($t(468) = -6.09$, $p < 0.01$) (Fig. 6), which further illustrates how the topography of normalized entropy can be modulated by clinical factors.

Using a second cohort for replication (see Methods), the fluctuation of the first value of the PC across time was performed. As previously observed, there was no increase across the three time points while it was the case for the entropy level (Supplementary Fig. 6A). Similar results were found when comparing entropy across time, which demonstrates a distinction between patients and controls (Supplementary Fig. 6B) and the fluctuation within-network across time (Supplementary Fig. 6C).

4. Discussion

In the current study we applied an edge-centric approach to a longitudinal stroke patient dataset. The analysis revealed a relation between the highest values of co-fluctuation with stroke severity and correlated with the number of domains recovered. Furthermore, normalized entropy was shown to increase across patient recovery time, suggesting a potential utility as an indication of recovery. Moreover, the normalized entropy was shown to differentiate patients according to the lesion location. Lastly, the participation coefficient's significant relation with stroke metrics adds another useful metric for further exploration. Collectively, this series of edge-centric network analyses demonstrate a novel direction for mapping the brain in a clinical setting. These analyses could potentially point towards improving diagnostic and treatment planning strategies.

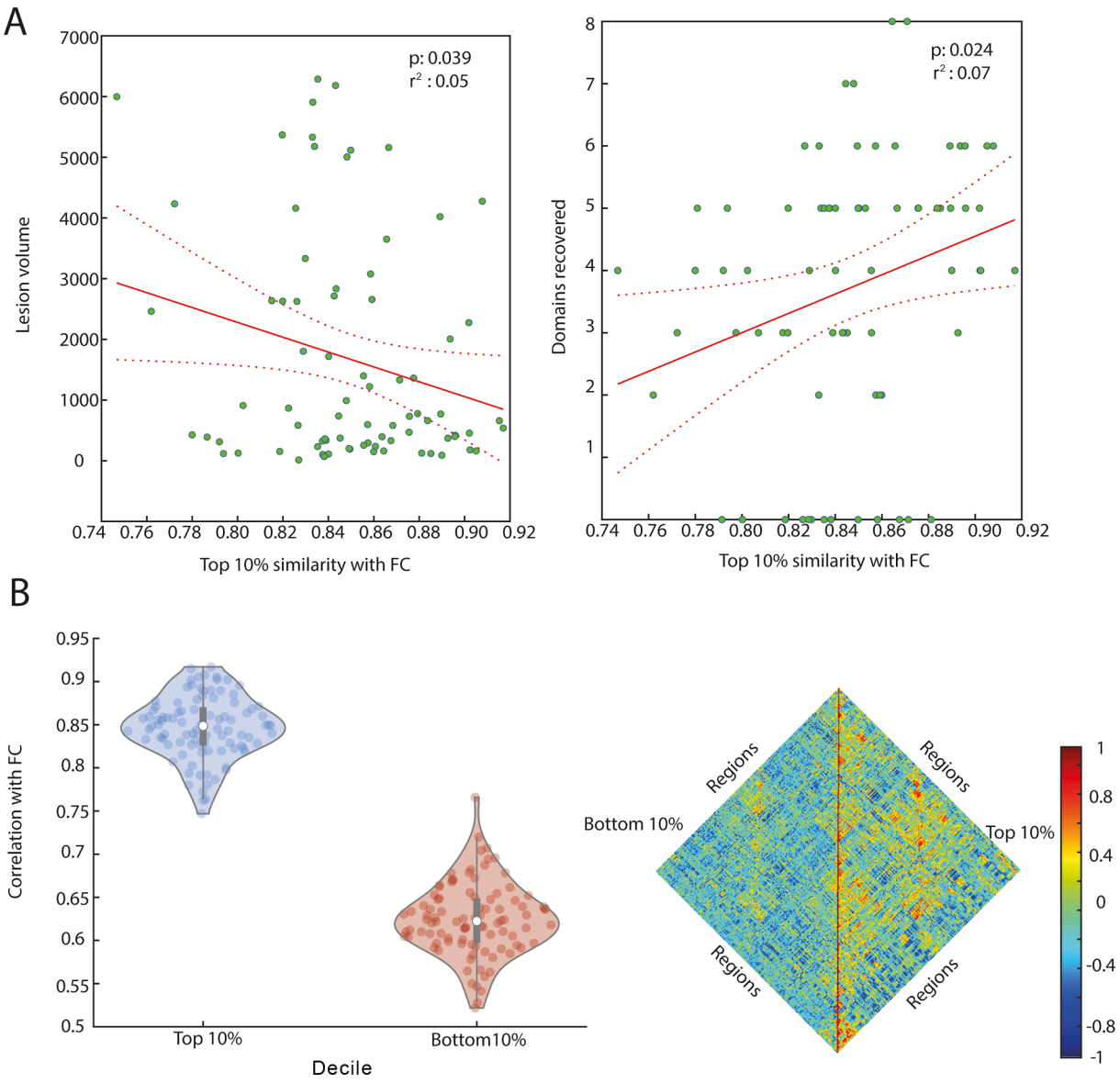

Fig. 5. High amplitude informative value: (A) Association between the 10% highest value of each patient with their corresponding (left) lesion volume and (right) amount of domains recovered after a year. (B) Comparison between the top and the bottom 10% FC.

4.1. Discussion of results

We employ an edge-centric analysis to calculate the normalized entropy of each node (Faskowitz et al., 2020) across stroke recovery. First, we show that the global average of this measure changes across time differently in our stroke sample, relative to the matched healthy control sample (Fig. 3a). Furthermore, these changes in normalized entropy are differentially expressed within a set of canonical functional networks (Schaefer et al., 2018) (Fig. 3c). Regarding the localization of the entropy level, previous studies associated the highest levels of entropy to specific networks (e.g., dorsal-attention or visual networks; (Faskowitz et al., 2020)). In this study we found that the difference between patients and healthy controls (i.e., where patients displayed more evenly distributed edge communities) is localized around the somatosensory cortices for the first two time points, whereas this difference is more diffuse in the third time point. We could speculate that as the stroke recovery process unfolds, edge community patterns might reconfigure in a way to promote globally higher entropies. It could be the case that in recovery, edge communities span many nodes more evenly, possibly creating higher entropy at more nodes.

It is important to account for the fact that BOLD signal is an indirect measure, reliant on diverse assumptions, and subject to many different sources of noise (Veldsman et al., 2015). Furthermore, another factor to take into consideration is the neurovascular coupling disruption produced by stroke (Lin et al., 2011). Therefore, the entropy increase across time could reflect the vascular coupling stabilization, potentially signaling a return to pre-stroke levels, as seen in previous literature (Blicher et al., 2012). Nevertheless, it is proposed that in order to study stroke populations, resting-state fMRI is better suited than event-related fMRI (Veldsman et al., 2015). This is due to its capacity to expose network-based pathology beyond the lesion site.

While analyzing the individual normalized entropy scores at the first time point, no significant relationship was found between the patients' globally averaged normalized entropy and stroke metrics. Nevertheless, previous studies showed a strong relationship between this measure and participation coefficient (Faskowitz et al., 2020). It has been found that stroke lesions with damaged gray matter regions and high participation coefficient, had a weak association with cognitive outcomes (Reber et al., 2021; Warren et al., 2014). Previous studies have shown that participation coefficient reflects, at an areal level, the balance between

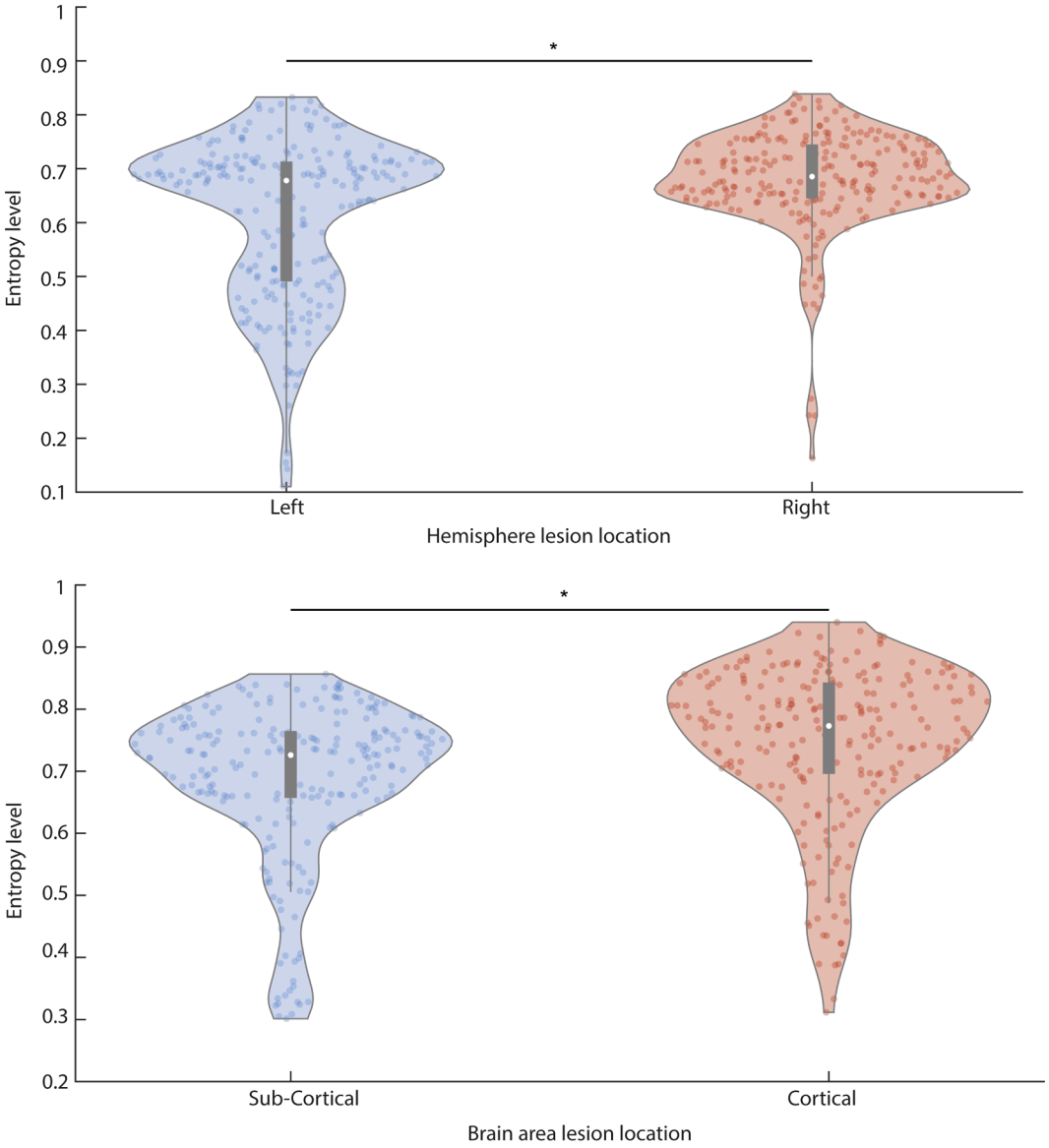

Fig. 6. Entropy level according to lesion location: Comparison in entropy level according to (top) the injured hemisphere and (bottom) the brain area (sub-cortical vs cortical).

intra- and inter-modular connections (Sporns et al., 2007). As participation coefficient was shown to be significantly related with edge community entropy (Faskowitz et al., 2020), we used the measure here to relate to the aforementioned stroke metrics. We found that the participation coefficient was related with the lesion volume and the NIHSS score, revealing its connection with the post-stroke effects. However, in contrast to normalized entropy, we did not find an increasing trend across time of participation coefficient, exposing one limitation of this specific metric. The fact that normalized entropy correlated with NIHSS score in the expected direction of the effect but not in a significant way, opens the door to debate if the metric might not be beneficial for this specific brain disorder. One possibility would be that participation coefficient is only applied to positive weights whereas the normalized entropy is based in edge communities that annotate all edges regardless of their sign. In order to answer this question, further studies should be developed using other clinical populations to demonstrate the relation between their severity metrics and normalized entropy and/or participation coefficient.

Previously, studies have tried to localize the spatial components of normalized entropy. In those studies, the brain systems associated with the highest levels of normalized entropy included visual, attentional, somatomotor and temporoparietal systems (Faskowitz et al., 2020). These findings were replicated in another study finding that overlap is greatest in primary sensory and attentional systems and lowest in association cortices (Jo et al., 2021b). The current study is the first one to examine the distinct entropy pattern regarding stroke lesion by comparing subjects with lesions in different hemispheres (left vs right) and lesion depth (cortical vs subcortical). The findings presented here open the way for further research to explore the use of these metrics to explore brain organization of this disorder.

4.2. *Relationship to other methods*

One of the most used techniques to relate neurological symptoms to specific brain areas involves identifying overlap in lesion location across patients with similar disorders. This approach, also known as lesion mapping, has been used profitably for decades, making it a reliable source of information for stroke patients diagnostics, treatment, and recovery prediction (Boes, 2015). The primary advantage of this method is that it is sensitive to even small and hyperacute infarction, and can be

used to assess if a certain brain region is necessary for a given cognitive function (Karnath et al., 2018; Sperber and Karnath, 2018). Nevertheless, the method could also be limited when the symptoms are not dependent on damage to a single brain region (Boes, 2015). Functional network metrics complement the anatomical features used in the clinic for decades, by adding dynamical and connectional components to study the global effect of the lesions, instead of just a local one. Relations between areas that before were believed to not be connected, could reveal influence on each other by being connected indirectly.

Recent works has shifted the attention from regions to networks damaged under stroke circumstances (Boes, 2015). Along these lines, we explore the edge-centric brain dynamics and its fluctuation across time in the different functional networks (Fig. 3c). The shift from node communities to edge communities provides a novel, and complementary, approach to inspect the brain dynamics in a disorder that not only affects the brain locally, but globally. In order to compare the obtained results with existing literature of the field, we analyze widely used metrics from a previous study (Pustina et al., 2017) and assessed their modulation across time (Sup. Fig. 8). As the current study uses functional data, a threshold was needed to calculate these corresponding network metrics.

One of the metrics used in this study, normalized entropy, was previously compared to other measures of overlap, like flexibility and versatility (Bassett et al., 2011; Betzel et al., 2020; Faskowitz et al., 2020; Shinn et al., 2017). Furthermore, a previous study linked structural lesions in simulated stroke networks by measuring the diversity of weights at each node (Saenger et al., 2018). Here, we added to this understanding by constructing a topographic map of entropies derived from the range of edge community affiliations at each node. The entropy metric here provides a time-averaged index of the diversity of dynamic edge co-fluctuation patterns emanating from each node. Future work should focus on the intersection between these dynamic patterns and the underlying anatomical structure (Davison et al., 2015; Liu et al., 2021), particularly in a clinical context.

Previous literature introduced related approaches such as quasi-periodic patterns (QPPs), which represent repeating spatiotemporal patterns of neural activity of predefined temporal length (Adhikari et al., 2020). The QPP involves propagation of activity in the default mode and task positive networks of the brain (Abbas et al., 2019). As in similar approaches (Petridou et al., 2013) they require picking a seed for its analysis, adding a subjective component to the process in contrast to the edge-centric approach which requires no seed. A similar technique showed that fMRI signals could be represented by a sparse spatiotemporal point process where the inflection points contained most of the signal's information (Cifre et al., 2020) in a similar way as presented in the high amplitude co-fluctuations on this study.

Previous studies proposed the use of obtained fine-scale dynamics by observing brief and intermittent episodes of high-amplitude co-fluctuations involving large sets of brain regions (Rabuffo et al., 2021; Zamani Esfahlani et al., 2020). In a similar way, a common approach to extract and cluster voxel- or vertex level activity during high-activity frames is the co-activation patterns, also known as CAPs (Karahanoglu and Van De Ville, 2015; Liu and Duyn, 2013). It is relevant to mention that while RSS co-fluctuations and CAPs are similar in some ways, our method is nonetheless distinct and has unique advantages. Most importantly, our method is built upon a mathematically exact decomposition of static rsFC into its frame-wise contributions. This decomposition enables us to quantify, precisely, how individual time points impact static rsFC. Furthermore, our method does not rely on sliding time windows nor step-size parameters. Even more, the decomposition does not require that we select a seed region or brain system in advance. Rather, our decomposition method considers all activity levels and the entire network simultaneously (Liu et al., 2021; Zamani Esfahlani et al., 2020). These studies show how dynamic information could be utilized to analyze case-control differences in a clinical neuroimaging setting.

Nevertheless, a remaining open question concerns the neurobiology underlying high-amplitude co-fluctuations, and how the resultant topography of the observed changes relates to stroke recovery at the neurological level. On one hand, their infrequent occurrence could reflect a dynamic strategy for limiting the consumption of metabolic resources. On the other hand, high-amplitude frames are suggested to be, to some extent, a mathematical necessity emerging in correlated, modular systems (Novelli and Razi, 2021). Another study presented a generative model for high-amplitude co-fluctuations in silico using computational simulations of whole-brain dynamics and demonstrated that such high-amplitude patterns have an origin in modular structural connections (Pope et al., 2021). This leads to the suggestion that these intermittent events are partly shaped by modular organization of structural connectivity indicating a potential overlap of functional and structural information (Liu et al., 2021; Pope et al., 2021; Rabuffo et al., 2021; van Oort et al., 2018). There is a concern that the high-amplitude co-fluctuations in the cortical activity that drive the nFC could be artifacts, potentially specific to fMRI. This has been mitigated by evidence showing that the high-amplitude events in the RSS of the edge time series are not systematically related to confounding variables including in-scanner motion, respiratory and heart rate (Zamani Esfahlani et al., 2020), and they readily appear in computational simulations (Pope et al., 2021; Rabuffo et al., 2021; Wang et al., 2018).

Based on these conclusions, we performed the analysis using this approach and we found how the highest ten percent of the data values, (sorted based on the RSS co-fluctuations) not only were associated with the lesion volume after stroke but also related to the number of cognitive domains in the patients' recovery (Fig. 5). The ability to inform about the recovery of the subjects suggest that the information contained in this subset of the data could be more explanatory than previously believed.

While its contributions compared to the nFC are still debated, it has been proposed that the RSS peaks not only occur when the Euclidean norm of the BOLD signal is large but, most likely, when the expressed spatial mode is well aligned with the leading eigenvector of the nFC. The leading eigenvector of the static nFC matrix could also be obtained as the first component of the BOLD activity, being mathematically equivalent (Novelli and Razi, 2021). The fluctuation across time of the first principal component value at each time point and the edge-centric derived metrics (top amplitude co-fluctuations and normalized entropy) reveals how the first two maintain consistency across time while the third has an increasing trend across time (Fig. 2). The similarities between the edge-centric approach and the principal components analysis of the node-centric approach reveal the strengths of the first one such as its simplicity or not needing any assumption used in sliding-window approaches (Novelli and Razi, 2021; van Oort et al., 2018). The normalized entropy fluctuation across time could refine our theoretical understanding of the patients' recovery after suffering a stroke.

4.3. Limitations

The current study investigates a stroke population using resting-state fMRI data. It is worth noting that stroke patients tend to be older than the usual populations where the assumptions of neurovascular coupling and the typical analysis pipelines are based (Veldsman et al., 2015). Additionally, the presented results should be interpreted given the caveat that the BOLD signal is not a direct measure of neuronal activity. Changes in network dynamics across timepoints thus reflect changes in observable BOLD fluctuations, but not necessarily nor specifically changes in neuronal dynamics.

Even though Figure S9 shows possible variation in the results, an assumption of the bootstrap procedure is that population variation can be estimated from resampling from the available data. However, the present dataset contains in general relatively small lesions. With this in mind, we note that we are not able to make a confident prediction about how these results could be extrapolated to a dataset consisting of patients with larger lesions.

The edge-centric approach involves a much larger dimensionality than the most-common node-centric methods. In particular, clustering a full eFC matrix, of size edge-by-edge, is impractical on personal computing hardware. To circumvent this, the edge time series, of size edge-by-time, can be clustered directly using k-means. However, this computational "shortcut" precludes the usage of other community detection methods, such as modularity maximization that operate on networked data (i.e., a "square" adjacency matrix).

Furthermore, the interpretation of the edge-community structure remains open to interpretation, and the cognitive relevance of these communities has yet to be established. Lastly, throughout this study, the comparison of functional signals was done in an undirected manner. Measures such as correlation cannot determine the directionality of influence between signals.

Further studies could analyze the effect of these metrics in asymmetrical networks to benefit from its directionality, such as the ones used in effective connectivity.

4.4. Future directions

Even if the current study is not focused on improving predictability of stroke recovery, we provide novel fMRI connectivity methods that could be used in the future for that purpose. Given that the eFC matrix can be employed to boost the identifiability of fMRI data (Jo et al., 2021a), future work could explore if similar improvements to predictive models could be obtained using eFC and related edge-centric data structures.

Recent literature has developed strategies to combine different data modalities (anatomical, functional, behavior, etc.) of stroke patients (Iorga et al., 2021; Kristinsson et al., 2021; Pustina et al., 2017). While this study does not include anatomical information of the patients, future multimodal studies could adapt the presented methods to include the structural constraints of each individual subject.

The current study demonstrates that relations derived from computational and theoretical research on the human connectome can help to advance our understanding of how focal brain lesions are modulated across time. Additionally, these data show the emerging possibility of how network neuroscience and connectomics can contribute to clinical advances. By using the same techniques, future studies could try to replicate these results by studying similar brain disorders in which a typical recovery pattern is expected.

The inclusion of animal models could also add more robustness to the edge-centric approach providing a natural bridge for testing external manipulations and measuring how these metrics are affected by different system complexities. Furthermore, computational models could contribute to this goal by simulating whole-brain connectivity and adding additional information of network interactions.

4.5. Conclusion

In conclusion, this study added new evidence for the role of the edge-centric approach as a promising bridge between structure and function. Also, it revealed how edge-centric analysis provides indicators that relate to lesion severity and reveal lesion recovery, making it the first study taking an edge-centric approach with clinical applications across time.

Code availability

Code to replicate the analysis and figures in this article is available at https://github.com/SebastianIdesis/Edge_Centric_Stroke_Recovery.

Funding

S.I is supported by the EU-project euSNN (MSCA-ITN-ETN. H2020-860563). G.D. is supported by the Spanish national research project (ref. PID2019-105772GB-I00/AEI/https://doi.org/10.13039/501100011033) funded by the Spanish Ministry of Science, Innovation and Universities (MCIU). This material is based upon work supported by the National Science Foundation under Grant No. 076059-00003C (RFB, JF, OS). MC was supported by FLAG-ERA JTC 2017 (grant ANR-17-HBPR-0001); MIUR – Departments of Excellence Italian Ministry of Research (MART_ECCELLENZA18_01); Fondazione Cassa di Risparmio di Padova e Rovigo (CARIPARO) – Ricerca Scientifica di Eccellenza 2018 – (Grant Agreement number 55403); Ministry of Health Italy Brain connectivity measured with high-density electroencephalography: a novel neurodiagnostic tool for stroke- NEUROCONN (RF-2008-12366899); Celeghin Foundation Padova (CUP C94I20000420007); BIAL foundation grant (No. 361/18); H2020 European School of Network Neuroscience- euSNN, H2020-SC5-2019-2, (Grant Agreement number 869505); H2020 Visionary Nature Based Actions For Heath, Wellbeing and Resilience in Cities (VARCITIES), H2020-SC5-2019-2 (Grant Agreement number 869505); Ministry of Health Italy: Eye-movement dynamics during free viewing as biomarker for assessment of visuospatial functions and for closed-loop rehabilitation in stroke – EYEMOVINSTROKE (RF-2019-12369300).

CRediT authorship contribution statement

Sebastian Idesis: Conceptualization, Formal analysis, Writing – review & editing. **Joshua Faskowitz:** Formal analysis, Writing – review & editing. **Richard F. Betzel:** Writing – review & editing. **Maurizio Corbetta:** Writing – review & editing. **Olaf Sporns:** Writing – review & editing. **Gustavo Deco:** Conceptualization, Writing – review & editing.

Declaration of Competing Interest

The authors declare that they have no known competing financial interests or personal relationships that could have appeared to influence the work reported in this paper.

Acknowledgments

We thank JC Griffis, NV Metcalf and GL Shulman for acquiring and pre-processing the data.

We thank Melina Timplalexi for assisting with the figures.

Appendix A. Supplementary data

Supplementary data to this article can be found online at https://doi.org/10.1016/j.nicl.2022.103055.

References

Abbas, A., Bassil, Y., Keilholz, S., 2019. Quasi-periodic patterns of brain activity in individuals with attention-deficit/hyperactivity disorder. Neuroimage Clin 21, 101653. https://doi.org/10.1016/j.nicl.2019.101653.

Adhikari, M.H., Belloy, M.E., Van der Linden, A., Keliris, G.A., Verhoye, M., 2020. Resting-state co-activation patterns as promising candidates for prediction of alzheimer's disease in aged mice. Front. Neural Circuits 14, 612529. https://doi.org/10.3389/fncir.2020.612529.

Ahn, Y.-Y., Bagrow, J.P., Lehmann, S., 2010. Link communities reveal multiscale complexity in networks. Nature 466 (7307), 761–764.

Allan, T.W., Francis, S.T., Caballero-Gaudes, C., Morris, P.G., Liddle, E.B., Liddle, P.F., Brookes, M.J., Gowland, P.A., Stamatakis, E.A., 2015. Functional connectivity in MRI is driven by spontaneous BOLD events. PLoS ONE 10 (4), e0124577.

Bassett, D.S., Sporns, O., 2017. Network neuroscience. Nat. Neurosci. 20 (3), 353–364. https://doi.org/10.1038/nn.4502.

Bassett, D.S., Wymbs, N.F., Porter, M.A., Mucha, P.J., Carlson, J.M., Grafton, S.T., 2011. Dynamic reconfiguration of human brain networks during learning. Proc. Natl. Acad. Sci. U.S.A. 108 (18), 7641–7646. https://doi.org/10.1073/pnas.1018985108.

Betzel, R., Cutts, S., Greenwell, S., Sporns, O., 2021. Individualized event structure drives individual differences in whole-brain functional connectivity. *bioRxiv*.

Betzel, R.F., Byrge, L., Esfahlani, F.Z., Kennedy, D.P., 2020. Temporal fluctuations in the brain's modular architecture during movie-watching. Neuroimage 213, 116687.

Blicher, J.U., Stagg, C.J., O'shea, J., Østergaard, L., MacIntosh, B.J., Johansen-Berg, H., Jezzard, P., Donahue, M.J., 2012. Visualization of altered neurovascular coupling in

chronic stroke patients using multimodal functional MRI. J. Cereb. Blood Flow Metab. 32 (11), 2044–2054.
Boes, C.J., 2015. History of neurologic examination books. Baylor University Medical Center Proceedings 28 (2), 172–179.
Brott, T., Adams Jr., H.P., Olinger, C.P., Marler, J.R., Barsan, W.G., Biller, J., Spilker, J., Holleran, R., Eberle, R., Hertzberg, V., et al., 1989. Measurements of acute cerebral infarction: a clinical examination scale. Stroke 20 (7), 864–870. https://doi.org/10.1161/01.str.20.7.864.
Chumin, E. J., Faskowitz, J., Esfahlani, F. Z., Jo, Y., Merritt, H. L., Tanner, J. C., Cutts, S. A., Pope, M. E., Sporns, O., Betzel, R., 2021. Cortico-Subcortical Interactions in Overlapping Communities of Edge Functional Connectivity. *bioRxiv*.
Cifre, I., Zarepour, M., Horovitz, S., Cannas, S.A., Chialvo, D.R., 2020. Further results on why a point process is effective for estimating correlation between brain regions. Papers in Phys. 12, 120003.
Corbetta, M., Ramsey, L., Callejas, A., Baldassarre, A., Hacker, C.D., Siegel, J.S., Astafiev, S.V., Rengachary, J., Zinn, K., Lang, C.E., Connor, L.T., Fucetola, R., Strube, M., Carter, A.R., Shulman, G.L., 2015. Common behavioral clusters and subcortical anatomy in stroke. Neuron 85 (5), 927–941. https://doi.org/10.1016/j.neuron.2015.02.027.
Corbetta, M., Siegel, J.S., Shulman, G.L., 2018. On the low dimensionality of behavioral deficits and alterations of brain network connectivity after focal injury. Cortex 107, 229–237. https://doi.org/10.1016/j.cortex.2017.12.017.
Crofts, J.J., Higham, D.J., Bosnell, R., Jbabdi, S., Matthews, P.M., Behrens, T., Johansen-Berg, H., 2011. Network analysis detects changes in the contralesional hemisphere following stroke. Neuroimage 54 (1), 161–169.
Davison, E.N., Schlesinger, K.J., Bassett, D.S., Lynall, M.-E., Miller, M.B., Grafton, S.T., Carlson, J.M., Hilgetag, C.C., 2015. Brain network adaptability across task states. PLoS Comput. Biol. 11 (1), e1004029.
Faskowitz, J., Esfahlani, F.Z., Jo, Y., Sporns, O., Betzel, R.F., 2020. Edge-centric functional network representations of human cerebral cortex reveal overlapping system-level architecture. Nat. Neurosci. 23 (12), 1644–1654. https://doi.org/10.1038/s41593-020-00719-y.
Faskowitz, J., Yan, X., Zuo, X.N., Sporns, O., 2018. Weighted stochastic block models of the human connectome across the life span. Sci. Rep. 8 (1), 12997. https://doi.org/10.1038/s41598-018-31202-1.
Fukushima, M., Betzel, R.F., He, Y., van den Heuvel, M.P., Zuo, X.-N., Sporns, O., 2018. Structure–function relationships during segregated and integrated network states of human brain functional connectivity. Brain Struct. Funct. 223 (3), 1091–1106.
Greenwell, S., Faskowitz, J., Pritschet, L., Santander, T., Jacobs, E. G., Betzel, R. F., 2021. High-amplitude network co-fluctuations linked to variation in hormone concentrations over menstrual cycle. *bioRxiv*.
Griffis, J.C., Metcalf, N.V., Corbetta, M., Shulman, G.L., 2019a. Structural disconnections contribute to lesion-induced brain functional connectivity disruptions via direct and indirect mechanisms. bioRxiv, 785576.
Griffis, J.C., Metcalf, N.V., Corbetta, M., Shulman, G.L., 2019b. Structural disconnections explain brain network dysfunction after stroke. Cell Rep. 28 (10), 2527–2540 e2529. https://doi.org/10.1016/j.celrep.2019.07.100.
Honey, C.J., Kötter, R., Breakspear, M., Sporns, O., 2007. Network structure of cerebral cortex shapes functional connectivity on multiple time scales. Proc. Natl. Acad. Sci. 104 (24), 10240–10245.
Honey, C.J., Sporns, O., Cammoun, L., Gigandet, X., Thiran, J.P., Meuli, R., Hagmann, P., 2009. Predicting human resting-state functional connectivity from structural connectivity. Proc. Natl. Acad. Sci. U.S.A. 106 (6), 2035–2040. https://doi.org/10.1073/pnas.0811168106.
Iorga, M., Higgins, J., Caplan, D., Zinbarg, R., Kiran, S., Thompson, C.K., Rapp, B., Parrish, T.B., 2021. Predicting language recovery in post-stroke aphasia using behavior and functional MRI. Sci. Rep. 11 (1), 1–12.
Jo, Y., Zamani Esfahlani, F., Faskowitz, J., Chumin, E.J., Sporns, O., Betzel, R.F., 2021a. The diversity and multiplexity of edge communities within and between brain systems. Cell Rep. 37 (7), 110032.
Jo, Y., Faskowitz, J., Esfahlani, F.Z., Sporns, O., Betzel, R.F., 2021b. Subject identification using edge-centric functional connectivity. Neuroimage 238, 118204.
Karahanoglu, F.I., Van De Ville, D., 2015. Transient brain activity disentangles fMRI resting-state dynamics in terms of spatially and temporally overlapping networks. Nat. Commun. 6, 7751. https://doi.org/10.1038/ncomms8751.
Karnath, H.-O., Sperber, C., Rorden, C., 2018. Mapping human brain lesions and their functional consequences. Neuroimage 165, 180–189.
Kristinsson, S., Zhang, W., Rorden, C., Newman-Norlund, R., Basilakos, A., Bonilha, L., Yourganov, G., Xiao, F., Hillis, A., Fridriksson, J., 2021. Machine learning-based multimodal prediction of language outcomes in chronic aphasia. Hum. Brain Mapp. 42 (6), 1682–1698.
Lin, W., Hao, Q., Rosengarten, B., Leung, W., Wong, K., 2011. Impaired neurovascular coupling in ischaemic stroke patients with large or small vessel disease. Eur. J. Neurol. 18 (5), 731–736.
Liu, X., Duyn, J.H., 2013. Time-varying functional network information extracted from brief instances of spontaneous brain activity. Proc. Natl. Acad. Sci. U.S.A. 110 (11), 4392–4397. https://doi.org/10.1073/pnas.1216856110.
Liu, Z.-Q., Vázquez-Rodríguez, B., Spreng, R. N., Bernhardt, B. C., Betzel, R. F., Misic, B., 2021. Time-resolved structure-function coupling in brain networks. *bioRxiv*.
Lyden, P., Claesson, L., Havstad, S., Ashwood, T., Lu, M., 2004. Factor analysis of the National Institutes of Health Stroke Scale in patients with large strokes. Arch. Neurol. 61 (11), 1677–1680. https://doi.org/10.1001/archneur.61.11.1677.
Novelli, L., Razi, A., 2021. A mathematical perspective on edge-centric functional connectivity. *arXiv preprint arXiv:2106.10631*.
Olafson, E.R., Jamison, K.W., Sweeney, E.M., Liu, H., Wang, D., Bruss, J.E., Boes, A.D., Kuceyeski, A., 2021. Functional connectome reorganization relates to post-stroke motor recovery and structural and functional disconnection. Neuroimage 245, 118642. https://doi.org/10.1016/j.neuroimage.2021.118642.
Park, H.J., Friston, K., 2013. Structural and functional brain networks: from connections to cognition. Science 342 (6158), 1238411. https://doi.org/10.1126/science.1238411.
Petridou, N., Gaudes, C.C., Dryden, I.L., Francis, S.T., Gowland, P.A., 2013. Periods of rest in fMRI contain individual spontaneous events which are related to slowly fluctuating spontaneous activity. Hum. Brain Mapp. 34 (6), 1319–1329.
Pope, M., Fukushima, M., Betzel, R., Sporns, O., 2021. Modular origins of high-amplitude co-fluctuations in fine-scale functional connectivity dynamics. *bioRxiv*.
Pustina, D., Coslett, H.B., Ungar, L., Faseyitan, O.K., Medaglia, J.D., Avants, B., Schwartz, M.F., 2017. Enhanced estimations of post-stroke aphasia severity using stacked multimodal predictions. Hum. Brain Mapp. 38 (11), 5603–5615.
Rabuffo, G., Fousek, J., Bernard, C., Jirsa, V., 2021. Neuronal cascades shape whole-brain functional dynamics at rest. *bioRxiv*, 2020.2012. 2025.424385.
Reber, J., Hwang, K., Bowren, M., Bruss, J., Mukherjee, P., Tranel, D., Boes, A.D., 2021. Cognitive impairment after focal brain lesions is better predicted by damage to structural than functional network hubs. PNAS 118 (19).
Rubinov, M., Sporns, O., 2010. Complex network measures of brain connectivity: uses and interpretations. Neuroimage 52 (3), 1059–1069. https://doi.org/10.1016/j.neuroimage.2009.10.003.
Rubinov, M., Sporns, O., 2011. Weight-conserving characterization of complex functional brain networks. Neuroimage 56 (4), 2068–2079. https://doi.org/10.1016/j.neuroimage.2011.03.069.
Saenger, V.M., Ponce-Alvarez, A., Adhikari, M., Hagmann, P., Deco, G., Corbetta, M., 2018. Linking entropy at rest with the underlying structural connectivity in the healthy and lesioned brain. Cereb. Cortex 28 (8), 2948–2958. https://doi.org/10.1093/cercor/bhx176.
Schaefer, A., Kong, R., Gordon, E.M., Laumann, T.O., Zuo, X.N., Holmes, A.J., Eickhoff, S. B., Yeo, B.T.T., 2018. Local-global parcellation of the human cerebral cortex from intrinsic functional connectivity MRI. Cereb. Cortex 28 (9), 3095–3114. https://doi.org/10.1093/cercor/bhx179.
Shinn, M., Romero-Garcia, R., Seidlitz, J., Vasa, F., Vertes, P.E., Bullmore, E., 2017. Versatility of nodal affiliation to communities. Sci. Rep. 7 (1), 4273. https://doi.org/10.1038/s41598-017-03394-5.
Siegel, J.S., Ramsey, L.E., Snyder, A.Z., Metcalf, N.V., Chacko, R.V., Weinberger, K., Baldassarre, A., Hacker, C.D., Shulman, G.L., Corbetta, M., 2016. Disruptions of network connectivity predict impairment in multiple behavioral domains after stroke. Proc. Natl. Acad. Sci. U.S.A. 113 (30), E4367–E4376. https://doi.org/10.1073/pnas.1521083113.
Siegel, J.S., Seitzman, B.A., Ramsey, L.E., Ortega, M., Gordon, E.M., Dosenbach, N.U.F., Petersen, S.E., Shulman, G.L., Corbetta, M., 2018. Re-emergence of modular brain networks in stroke recovery. Cortex 101, 44–59. https://doi.org/10.1016/j.cortex.2017.12.019.
Silasi, G., Murphy, T.H., 2014. Stroke and the connectome: how connectivity guides therapeutic intervention. Neuron 83 (6), 1354–1368.
Sperber, C., Karnath, H.-O., 2018. On the validity of lesion-behaviour mapping methods. Neuropsychologia 115, 17–24.
Sporns, O., Faskowitz, J., Teixeira, A.S., Cutts, S.A., Betzel, R.F., 2021. Dynamic expression of brain functional systems disclosed by fine-scale analysis of edge time series. Network Neurosci. 5 (2), 405–433.
Sporns, O., Honey, C.J., Kötter, R., Kaiser, M., 2007. Identification and classification of hubs in brain networks. PLoS ONE 2 (10), e1049.
Tagliazucchi, E., Balenzuela, P., Fraiman, D., Chialvo, D.R., 2012. Criticality in large-scale brain FMRI dynamics unveiled by a novel point process analysis. Front. Physiol. 3, 15. https://doi.org/10.3389/fphys.2012.00015.
Tzourio-Mazoyer, N., Landeau, B., Papathanassiou, D., Crivello, F., Etard, O., Delcroix, N., Mazoyer, B., Joliot, M., 2002. Automated anatomical labeling of activations in SPM using a macroscopic anatomical parcellation of the MNI MRI single-subject brain. Neuroimage 15 (1), 273–289.
van Oort, E.S., Mennes, M., Schröder, T.N., Kumar, V.J., Jimenez, N.I.Z., Grodd, W., Doeller, C.F., Beckmann, C.F., 2018. Functional parcellation using time courses of instantaneous connectivity. Neuroimage 170, 31–40.
Veldsman, M., Cumming, T., Brodtmann, A., 2015. Beyond BOLD: optimizing functional imaging in stroke populations. Hum. Brain Mapp. 36 (4), 1620–1636.
Wang, S.H., Lobier, M., Siebenhühner, F., Puoliväli, T., Palva, S., Palva, J.M., 2018. Hyperedge bundling: A practical solution to spurious interactions in MEG/EEG source connectivity analyses. Neuroimage 173, 610–622.
Wang, X., Seguin, C., Zalesky, A., Wong, W.-W., Chu, W.-C.-W., Tong, R.-K.-Y., 2019. Synchronization lag in post stroke: relation to motor function and structural connectivity. Network Neurosci. 3 (4), 1121–1140.
Warren, D.E., Power, J.D., Bruss, J., Denburg, N.L., Waldron, E.J., Sun, H., Petersen, S.E., Tranel, D., 2014. Network measures predict neuropsychological outcome after brain injury. Proc. Natl. Acad. Sci. 111 (39), 14247–14252.
Wodeyar, A., Cassidy, J.M., Cramer, S.C., Srinivasan, R., 2020. Damage to the structural connectome reflected in resting-state fMRI functional connectivity. Network Neurosci. 4 (4), 1197–1218.
Zamani Esfahlani, F., Jo, Y., Faskowitz, J., Byrge, L., Kennedy, D.P., Sporns, O., Betzel, R. F., 2020. High-amplitude cofluctuations in cortical activity drive functional connectivity. Proc. Natl. Acad. Sci. U.S.A. 117 (45), 28393–28401. https://doi.org/10.1073/pnas.2005531117.
Zandieh, A., Kahaki, Z.Z., Sadeghian, H., Pourashraf, M., Parviz, S., Ghaffarpour, M., Ghabaee, M., 2012. The underlying factor structure of National Institutes of Health Stroke scale: an exploratory factor analysis. Int. J. Neurosci. 122 (3), 140–144. https://doi.org/10.3109/00207454.2011.633721.